BIOCHEMISTRY
including biophysical chemistry & molecular biology
Article

*Biochemistry* **2010,** *49,* 1495–1506 1495
DOI: 10.1021/bi901609m

# Steady-State Kinetic Characterization of Kinase Activity and Requirements for $Mg^{2+}$ of Interleukin-1 Receptor-Associated Kinase-4

Mohammad Hekmat-Nejad,* Terrence Cai, and David C. Swinney

*Department of Virology, Roche Palo Alto, LLC, 3431 Hillview Avenue, Palo Alto, California 94304*

*Received September 15, 2009; Revised Manuscript Received November 17, 2009*

ABSTRACT: Interleukin-1 receptor-associated kinase-4 (IRAK-4) is a Ser/Thr-specific protein kinase that plays a critical role in intracellular signaling cascades mediated by Toll-like and interleukin-1 (IL-1) receptors. Despite a growing body of information on the physiological functions of IRAK-4, its kinase activity remains poorly studied. The present study entails characterization of the steady-state kinetic properties and $Mg^{2+}$ requirements of full-length, recombinant human IRAK-4 preactivated by incubation with MgATP. In the presence of 20 mM $Mg^{2+}$, activated IRAK-4 herein is demonstrated to phosphorylate a peptide substrate (IRAK-1 peptide), derived from the activation loop of IRAK-1, with a $k_{cat}$ of $30 \pm 2.9$ $s^{-1}$ and $K_m$ values of $668 \pm 120$ and $852 \pm 273$ $\mu$M for ATP and the peptide, respectively. Two-substrate, dead-end and product inhibition data, using analogues of ATP, are consistent with both a sequential ordered kinetic mechanism with ATP binding to the enzyme prior to the peptide and a sequential random mechanism. Investigation of the $Mg^{2+}$ requirements for phosphoryl transfer activity of IRAK-4 revealed that more than one $Mg^{2+}$ ion interacts with the enzyme and that the enzyme is maximally active in the presence of 5−10 mM free $Mg^{2+}$. While one divalent metal, as part of a chelate complex with ATP, is essential for catalysis, kinetic evidence is provided to show that uncomplexed $Mg^{2+}$ further enhances the catalytic activity of IRAK-4 by bringing about an ~3-fold increase in $k_{cat}$ and an ~6-fold reduction in the $K_m$ for ATP and by rendering the interaction between the nucleotide and peptide substrate binding sites less antagonistic.

Members of the interleukin-1 receptor-associated kinase (IRAK)[1] family are emerging as important regulators of innate immunity and inflammation. The human IRAK family is comprised of four members, IRAK-1, IRAK-2, IRAK-M, and IRAK-4 (*1*). IRAK-4, a Ser/Thr-specific protein kinase, is the most recently discovered member of the IRAK family (*2*). There is growing evidence in support of IRAK-4 performing a pivotal function in signaling pathways triggered by stimulation of Toll-like and the proinflammatory interleukin-1 family of receptors (TLR and IL-1R, respectively). Patients with defective IRAK-4 exhibit deficiencies in TLR signaling and production of proinflammatory cytokines. IRAK-4 knockout cell lines and mouse are unresponsive to stimulation by IL-1 and various TLR ligands (*3*−*5*). Other lines of evidence include studies demonstrating compromised IL-1-triggered signaling in cells overexpressing IRAK-4 proteins with truncated kinase domains (*6*). Given the critical role IRAK-4 plays in regulating inflammatory processes, it has attracted attention as a potential target for novel anti-inflammatory therapeutics (*7*, *8*).

*To whom correspondence should be addressed. Phone: 650-855-5682. Fax: 650-852-1700. E-mail: mohammad.hekmat-nejad@roche.com.

[1]Abbreviations: IRAK, interleukin-1 receptor-associated kinase; TNF-α, tumor necrosis factor α; NFκB, nuclear factor κB; TLR, Toll-like receptor; IL-1R, interleukin-1 receptor; TRAF6, TNF-α receptor-associated factor 6; JNK, c-Jun $NH_2$-terminal kinase; IKK, IκB kinase; AP-1, activating protein-1; MAPK, mitogen-activated protein kinase; HEPES, *N*-(2-hydroxyethyl)piperazine-*N*′-2-ethanesulfonic acid; DTT, dithiothreitol; EDTA, ethylenediaminetetraacetic acid; EGTA, ethylene glycol tetraacetic acid; PEP, phosphoenolypyruvic acid.

Genetic and biochemical studies have begun to unravel the molecular mechanisms underlying IRAK-4's function in IL-1-stimulated signal transmission. Upon stimulation of IL-1R, IRAK-4 and IRAK-1 are recruited to the activated receptor complex (*9*). After undergoing activation through a poorly understood mechanism, IRAK-4 phosphorylates IRAK-1 on serine and threonine residues within its activation loop. These initial IRAK-4-dependent phosphorylation events trigger kinase activity of IRAK-1 which in turn results in autophosphorylation of several residues in a region outside of IRAK-1's kinase core (*10*). Hyperphosphorylated IRAK-1 subsequently dissociates from the receptor complex to interact with the downstream adaptor molecule TNF-α receptor-associated factor 6 (TRAF6). The release of TRAF6-bound IRAK-1 sets in motion a number of downstream signaling events involving IκB kinases (IKKs) and mitogen- and stress-activated protein kinases (MAPKs) such as c-Jun N-terminal kinase (JNK) and p38 that ultimately result in activation of transcription factors NF-κB and AP1.

The requirement for kinase activity of IRAK-4 in cell signaling remains a subject of investigation. Earlier work has shown that kinase-deficient IRAK-4 is dominant negative and its overexpression results in strong inhibition of IL-1-induced signaling in HEK293 cells, suggesting that the kinase activity of IRAK-4 is essential for its signaling function (*2*). Recent *in vivo* studies, using IRAK-4 kinase-deficient knock-in mice, have further confirmed a critical role for catalytic activity of IRAK-4 (*11*). However, these findings have been repudiated by other studies showing restoration of IL-1 signaling by a kinase-dead IRAK-4 in IRAK-4 deficient human fibroblast cells, thus suggesting that the kinase activity of IRAK-4 may be dispensable or redundant


Published on Web 01/27/2010

with IRAK-1 in the IL-1-driven signaling pathway (*12*). Similarly, studies by Song et al., using genetic complementation and IRAK selective small molecule inhibitors, have shown that inhibition of both IRAK-1 and IRAK-4 is required to block IL-1-mediated cytokine production in human endothelial cells, thus indicating redundancy in the pathway (*13*).

Similar to other IRAKs, IRAK-4 is a multidomain protein consisting of an N-terminal death domain, implicated in mediating interaction with adapter proteins, followed by a linker region of unknown structure and function and a C-terminal kinase domain. The kinase domain of IRAK-4 bears <32% sequence identity to other kinases in the human kinome (*14*). The X-ray crystal structure of the kinase domain of IRAK-4, in an activated state, has been solved (*14*, *15*). Comparing the structure of the IRAK-4 kinase core with those of other kinases revealed several conserved features as well as elements that appear to be unique to this enzyme. Specifically, in IRAK-4, the peptide substrate binding pocket appears to be more open compared to other kinases, the ATP pocket contains a nontypical gatekeeper residue, Tyr 262, and the N-terminal lobe bears a unique extension. It is not known whether these distinctive structural features confer novel functional properties to IRAK-4. To answer this question and to help clarify the role that the kinase activity of IRAK-4 plays in cell signaling, it is necessary to characterize its catalytic properties. Studies presented here were carried out to determine the steady-state kinetic parameters defining IRAK-4's kinase activity, to establish the kinetic mechanism for the phosphoryl transfer reaction, and to elucidate the role of the metal activator $Mg^{2+}$ in catalysis.

Confirming earlier results from Cheng and co-workers (*16*), herein we demonstrate that full-length, recombinant IRAK-4 can be activated *in vitro* by treatment with MgATP. Previous work had shown that both IRAK-1 protein and a synthetic peptide derived from its activation loop (IRAK-1 peptide, amino acids 359−389) can serve as substrates for the kinase activity of IRAK-4 *in vitro* (*2*). On the basis of these results, we chose the IRAK-1 activation loop peptide as the phospho-acceptor substrate for kinetic characterization of activated IRAK-4. Two-substrate kinetic data indicate that IRAK-4 phosphorylates IRAK-1 peptide via a sequential pathway. Dead-end and product inhibition results narrowed the possible kinetic mechanisms to strictly ordered, with ATP binding prior to the peptide substrate, or a random mechanism.

The steady-state kinetic studies described above were carried out in the presence of $Mg^{2+}$ maintained at a total and nonphysiological concentration of 20 mM. While most protein kinases require at least one divalent metal cation to function, several have been shown to interact with more than one metal cation and to exhibit different kinetic properties depending on the type and concentration of the divalent metal (*17*−*20*). These studies have raised the intriguing possibility that the catalytic function of protein kinases may be subject to regulation by fluxes in concentrations of metal activators. So far, each kinase appears to respond to the identity and concentration of the divalent ion in a different manner (*21*). Motivated to understand the role that $Mg^{2+}$ plays in the IRAK-4 reaction, in particular as a possible factor contributing to the efficiency with which IRAK-4 phosphorylates IRAK-1 peptide substrate, the effects of $Mg^{2+}$ on the kinetic properties of IRAK-4 were investigated. Kinetic evidence is presented to show that IRAK-4 requires more than one $Mg^{2+}$ for optimum activity. One $Mg^{2+}$ ion, in complex with ATP, is essential for the phosphoryl transfer reaction. The second, ATP-free $Mg^{2+}$ further contributes to the IRAK-4 reaction by reducing the $K_m$ for ATP, increasing $k_{cat}$, and by relieving the negative synergism between the nucleotide and peptide binding sites.

## MATERIALS AND METHODS

*General*. ATP was purchased from Roche Applied Sciences, Indianapolis, IN. ADP, AMPNP, Tween 20, γ-globulins from bovine blood (99% purity), β-nicotinamide adenine dinucleotide (reduced), phosphoenolpyruvic acid, rabbit muscle pyruvate kinase−lactate dehydrogenase, β-glycerol phosphate, sodium orthovanadate, EPPS, β-mercaptoethanol, EGTA, Brij 35, and $MgCl_2$ were obtained from Sigma-Aldrich, St. Louis, MO. Dithiothreitol was from Promega, Madison, WI. [γ-$^{33}$P]ATP (3000 Ci/mmol) was from GE Healthcare, Buckinghamshire, England. IRAK-1 activation loop peptide ($NH_2$-KKARFSRFAGSSPSQSSMVAR-COOH) was synthesized by CPC Scientific, San Jose, CA. A phosphorylated peptide carrying a phosphate on Ser 17 of the peptide substrate ($NH_2$-KKARFSRFAGSSPSQSpSMVAR-COOH) was made by AnaSpec, Fremont, CA. EDTA was from Mediatech, Herndon, VA. P81 phosphocellulose filter papers were obtained from Upstate Cell Signaling Solutions, Lake Placid, NY. Ready Safe liquid scintillation cocktail was from Beckman Coulter, Fullerton, CA.

*Expression and Purification of Recombinant IRAK-4*. Recombinant, full-length human IRAK-4 was expressed in *sf*9 insect cells with a hexahistidine tag at its N-terminus and purified, using metal affinity and gel filtration chromatography, in the same manner as previously described for a truncated IRAK-4 construct (*14*).

*In Vitro Activation of IRAK-4*. Activation of IRAK-4 was achieved by incubating purified IRAK-4 (final concentration of 3 μM) with 250 μM ATP, 20 mM $MgCl_2$ in 20 mM MOPS (pH 7.2), 25 mM β-glycerol phosphate, 5 mM EGTA, 1 mM sodium orthovanadate, and 1 mM DTT at room temperature for 4 h. The 4 h incubation was deemed adequate for fully activating IRAK-4 as judged by the kinase activity assay for measuring phosphorylation of IRAK-1 peptide. Subsequent to incubation with MgATP, the sample was concentrated using an Amicon concentrator with an YM30 membrane according to the manufacturer's recommendations. Concentrated protein was then filtered over a Gelman filter with 0.8 μm pore size. The clarified protein was run over a Superdex 200 column 26/60 using a buffer consisting of 50 mM HEPES (pH7.5), 10% glycerol, 300 mM NaCl, 10 mM β-mercaptoethanol, and 0.05% Brij 35. Fractions containing IRAK-4 were pooled, concentrated to 1 mg/mL, and stored at −80 °C. Activated IRAK-4 was used in all of the kinetic experiments unless stated otherwise.

*Kinase Activity Assay*. A radiometric, end point assay, using IRAK-1 peptide, was utilized for measuring the kinase activity of IRAK-4. All concentrations were final in the reaction mixture. The kinase assay was carried out in a volume of 40 μL of standard assay buffer containing 25 mM HEPES (pH 7.5), 170 mM NaCl, 20 mM $MgCl_2$, 0.01% Tween 20, 2 mM DTT, 0.1% bovine γ-globulins, [γ-$^{33}$P] ATP (50−4000 cpm/pmol), 0.08−5 mM unlabeled ATP, 0.04−2 mM peptide substrate, and 4 nM IRAK-4. Reactions were typically initiated by the addition of the enzyme, incubated for 20−30 min at 30 °C, and terminated by the addition of EDTA to a final concentration of 100 mM. A portion of terminated reactions (15 μL) was transferred to 2 × 2 cm$^2$ P81 phosphocellulose filter squares. After three washes of 10 min with

~4 mL of 0.75% phosphoric acid per filter square, the filter papers were dried and subsequently counted in the presence of 5 mL of scintillation fluid in a PerkinElmer Life Sciences Tri-Carb 1600TR counter. In preliminary experiments, aliquots of the reaction were analyzed for formation of the phosphopeptide at multiple time points ranging from 0 to 60 min and under different concentrations of the enzyme and the substrates. Product formation was shown to proceed linearly with time, and the initial rates of the reaction, determined from the slopes of progress curves, were shown to increase in direct proportion to the concentration of the enzyme.

*ATPase Assay*. Hydrolysis of ATP in the absence of the peptide substrate was measured using the pyruvate kinase−lactate dehydrogenase detection system that couples generation of ADP to oxidation of NADH (*22*). The reaction was carried out in the standard assay buffer employed in the phosphoryl transfer reaction to the peptide but without γ-globulins. Other components of the reaction included 0.49 mM NADH, 1.65 mM PEP, 0.5 μM IRAK-4, varying concentrations of ATP, and 4.5 and 5.5 units/mL pyruvate kinase and lactate dehydrogenase, respectively. Reactions were carried out in a volume of 100 μL in 96-well polystyrene clear plates at 30 °C. Changes in absorbance were monitored at 340 nm in a Molecular Device's SepctraMax Plus plate reader. ATPase rates changed linearly with concentration of IRAK-4 up to the highest concentration tested (0.5 μM).

*Effect of NaCl on Kinetic Parameters of IRAK-4*. Initial rates were measured as a function of varying concentrations of one substrate while the concentration of the second substrate was maintained at a constant value and in the presence of different concentrations of NaCl (20, 45, 70, 120, and 170 mM). With ATP as the variable substrate, the peptide was used at a concentration of 2 mM, while the concentration of the nucleotide was changed from 0.078 to 5 mM. With peptide as the variable substrate, the concentration of ATP was maintained at 5 mM, while the concentration of the peptide was changed from 0.1 to 2.25 mM. Apparent kinetic constants were extracted from a fit of the initial velocities to the Michaelis−Menten equation (eq 1; see below).

*Effect of Free $Mg^{2+}$ on Kinetics of IRAK-4*. Experiments on the effects of $Mg^{2+}$ concentration on the kinetic properties of IRAK-4 were carried out in a modified buffer consisting of 75 mM EPPS (pH 8.0), 0.01% Tween 20, 20 mM NaCl, and 0.1% bovine γ-globulins. The concentration of total $Mg^{2+}$ needed to achieve a desired concentration of free $Mg^{2+}$ was calculated using an association constant of 73 $mM^{-1}$ for the MgATP complex and the equation $[ATP]_{total} = [MgATP](1 + 1/K_a[Mg^{2+}]_{free}$, derived from the equation for MgATP association equilibrium ($K_a = [MgATP]/[ATP]_{free}[Mg^{2+}]_{free}$) and $[ATP]_{total} = [ATP]_{free} + [MgATP]$. In the equation, the concentrations of free $Mg^{2+}$ and total ATP were fixed, and the concentration of MgATP was treated as the unknown. The required concentration of total $Mg^{2+}$ was the sum of free $Mg^{2+}$ and MgATP concentrations. In calculating the concentration of total and free $Mg^{2+}$, the equilibrium between Na and ATP was not taken into consideration. Since the association constant for NaATP is significantly lower than that for MgATP (0.014 versus 73 $mM^{-1}$, respectively (*33*), it was assumed that the concentration of NaATP was negligible. The reactions were processed in exactly the same manner as the standard radiometric assay for phosphorylation of the peptide substrate described above.

*Substrate Analogue and Product Inhibition*. In order to find clues about the substrate binding order, mechanisms of inhibition studies with the nonhydrolyzable ATP analogue, AMPPNP, and ADP were carried out. In these experiments the concentration of one substrate was kept constant (close to its $K_m$) while the concentration of the second substrate was varied. When ATP was the varied substrate, its concentration was changed from 0.1 to 4 mM while the peptide was maintained at a concentration of 1.3 mM. When the peptide was used as the variable substrate, a concentration range of 0.1−2.5 mM with ATP kept at 0.8 mM was utilized. Inhibitors were preincubated with the enzyme at room temperature for 10 min prior to the start of the reaction with the substrates. The reactions were carried out and processed in the same fashion as the standard peptide phosphorylation assay.

*Data Analysis*. Initial velocity data were analyzed by nonlinear least-squares, using either Grafit, version 5.06, or GraphPad Prism, version 4.0, software packages. The Michaelis−Menten equation (eq 1) was used to obtain apparent kinetic constants.

$$v = \frac{V_{max}[S]}{K_m + [S]} \quad (1)$$

In this equation, $v$ and $V_{max}$ are the initial and maximum rates, respectively, and [S] is the varied substrate concentration with the corresponding Michaelis constant ($K_m$). Bisubstrate velocity data were fit to the kinetic equations for ternary complex (sequential, eq 2) and double-displacement (ping-pong, eq 3) mechanisms (*23*).

$$v = \frac{V_{max}[A][B]}{K_{ia}K_b + K_a[B] + K_b[A] + [A][B]} \quad (2)$$

$$v = \frac{V_{max}[A][B]}{K_a[B] + K_b[A] + [A][B]} \quad (3)$$

In eqs 2 and 3, [A] and [B] represent the substrate concentrations, $K_a$ and $K_b$ are the substrate Michaelis constants, and $K_{ia}$ is the dissociation constant for substrate A from free enzyme. The α factor (calculated as $K_a/K_{ia}$) is a measure of the degree to which the binding pockets for the substrates interact with one another (*23*). In order to check for deviations from ideal behavior, double-reciprocal plots of rate data were generated and analyzed by linear regression analysis. In the inhibition experiments, in addition to double-reciprocal plots, secondary plots of slope and intercept versus concentration of the inhibitor were generated and checked for linearity. Depending on the mode of inhibition, rate data from inhibition experiments were fit to the equations for competitive, noncompetitive, and uncompetitive mechanisms of enzyme inhibition (eqs 4−6 (*23*)).

$$v = \frac{V_{max}[S]}{K_m(1 + [I]/K_{is}) + [S]} \quad (4)$$

$$v = \frac{V_{max}[S]}{K_m(1 + [I]/K_{is}) + [S](1 + [I]/K_{ii})} \quad (5)$$

$$v = \frac{V_{max}[S]}{K_m + [S](1 + [I]/K_{ii})} \quad (6)$$

In these equations, [I] is the inhibitor concentration, $K_{is}$ represents the slope inhibition constant for the EI complex (enzyme−inhibitor binary complex), and $K_{ii}$ is the intercept inhibition constant for the EIS complex (enzyme−inhibitor−substrate ternary complex).

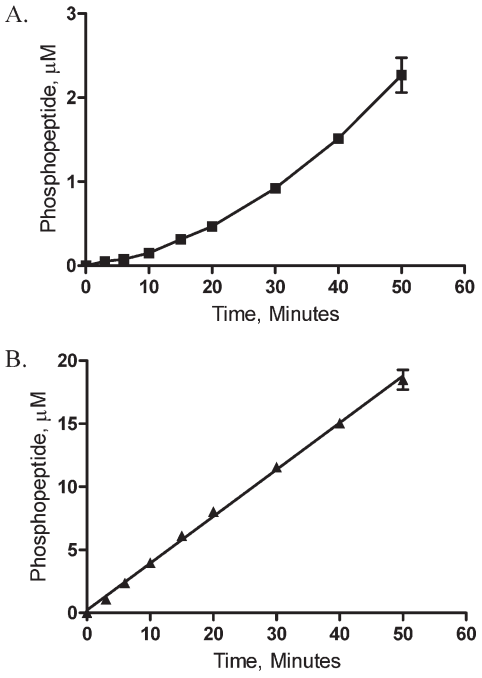


FIGURE 1: Progress curves for phosphorylation of IRAK-1 peptide by IRAK-4 prior to (A) and after (B) preincubation with ATP. Each reaction contained 5 nM IRAK-4, 0.8 mM ATP, and 0.25 mM peptide substrate.

Initial rate data with free $Mg^{2+}$ were processed first by fitting them to eq 2 for the sequential kinetic mechanism. The resulting kinetic parameters were subsequently plotted against the concentration of free $Mg^{2+}$. The apparent ATP $K_m$ ($_{app}K_{MgATP}$) was fit to eq 7 to calculate the $K_m$ values for ATP with only one $Mg^{2+}$ ion bound to the enzyme ($K_{MgATP}$), when two metal ions are bound to the enzyme ($K_{MgATP'}$), and the apparent affinity for $Mg^{2+}$ ($K_{Mg}$) (*23*, *24*).

$$_{app}K_{MgATP} = \frac{K_{MgATP'}[Mg^{2+}] + K_{MgATP}K_{Mg}}{[Mg^{2+}] + K_{Mg}} \quad (7)$$

## RESULTS

*In Vitro Activation of IRAK-4*. Kinetic characterization of full-length IRAK-4 in this study was carried out using a recombinant enzyme expressed in baculovirus insect cells and purified (>90%) by metal ion and size exclusion chromatography (data not shown). As shown in Figure 1A, during preliminary characterization of the catalytic activity of IRAK-4, it became apparent that formation of the phosphopeptide product is not linear with time and is distinguished by a lag before reaching a faster steady-state phase. While a number of factors could give rise to a curvilinear progress curve in an enzyme-catalyzed reaction, in the case of protein kinases, several examples have been documented showing activation of the kinase during the course of phosphorylation of the exogenously added phospho-acceptor substrate (*25*−*28*). Moreover, the mechanism underlying the activation process has been shown to involve autocatalyzed phosphorylation of the kinase on one or more residues in the activation loop. We hypothesized that the parabolic product formation curves of full-length IRAK-4 similarly arose from phosphorylation-mediated activation of the enzyme while it is phosphorylating the peptide substrate. Consistent with this hypothesis, pretreatment of the enzyme with MgATP not only had a linearizing effect on the reaction time course but also led to a 10−20-fold enhancement in the specific activity of the enzyme (Figure 1B). When IRAK-4 was incubated with ATP or $Mg^{2+}$ alone, no change in the catalytic activity was observed (data not shown), suggesting that the mechanism of activation with MgATP involves phosphorylation of the protein. Although the protein purified from insect cells appears not to be in a fully activated state, because its activity changes in the course of the phosphoryl transfer to the peptide substrate (see Figure 1A), it is difficult to determine with accuracy the degree to which pretreatment with MgATP activates the enzyme. Activated IRAK-4 generated in the present study yielded linear progress curves and initial velocity data that followed Michaelis−Menten kinetics, indicating that MgATP preactivation had rendered the enzyme suitable for kinetic characterization. All subsequent experiments in this study were carried out with enzyme that had been pretreated with MgATP and repurified by size exclusion chromatography.

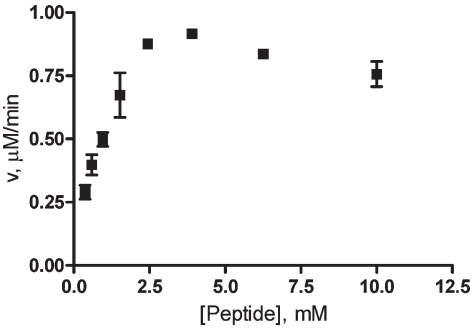


FIGURE 2: Variation in reaction velocity in response to varying concentrations of the peptide substrate. Initial velocities were measured using 4 nM IRAK-4, a subsaturating concentration of ATP (0.2 mM), and varying concentrations of IRAK-1 peptide.

*Two-Substrate Steady-State Kinetics*. Having prepared an activated and kinetically well-behaved IRAK-4 protein, we proceeded to characterize its steady-state kinetic properties. Specifically, we were interested in determining the steady-state kinetic constants and the kinetic mechanism defining the kinase activity of IRAK-4. To that end, the initial rates of the reaction were measured in response to varied concentrations of both substrates in the presence of 20 mM $Mg^{2+}$ and 170 mM NaCl. All velocity measurements corresponded to the initial rates during which time less than 10% of either substrate was turned over and the rate of the reaction changed linearly with the concentration of enzyme. As shown in Figure 2, the reaction deviates from Michaelis−Menten saturation kinetics at concentrations of the peptide substrate > 3 mM. Relative to the peak activity at 3 mM peptide, a loss of 9% and 18% in initial velocity was observed at 5 and 10 mM peptide, respectively. The cause of this apparent loss of activity at high peptide concentrations is unknown, and although direct inhibition by the peptide could have resulted in the diminution of enzymatic activity, other possible nonspecific mechanisms could not be ruled out. Subsequent to this finding, the steady-state rate measurements and analysis were limited to a peptide concentration range (typically < 3 mM) that yielded little or no inhibition and hyperbolic rate plots.

The kinetics of a bisubstrate enzyme-catalyzed reaction follows one of two general kinetic pathways: the ternary complex (sequential) or double displacement (ping-pong) (*23*, *29*). In order to distinguish between these two mechanisms and pick an appropriate kinetic model for analysis of the bisubstrate rate

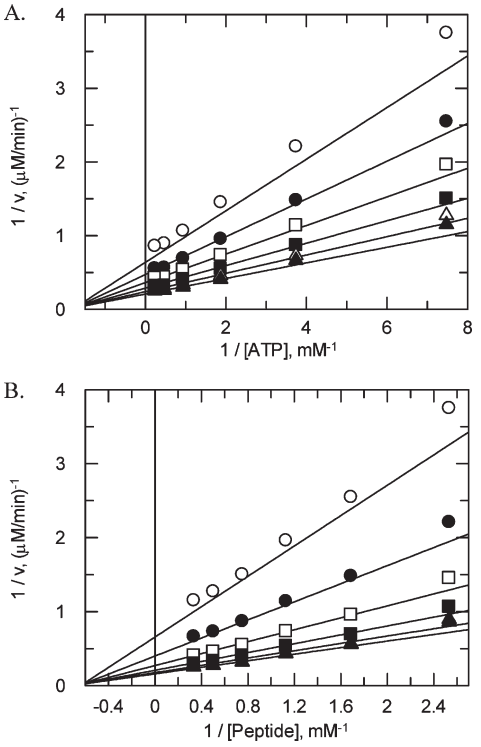


FIGURE 3: Two-substrate steady-state kinetics of IRAK-4. (A) Double-reciprocal plot of reaction velocity versus concentration of ATP. Initial rates were measured with 4 nM IRAK-4 as a function of varied concentrations of ATP and at six fixed concentrations of IRAK-1 peptide [0.395 (○), 0.593 (●), 0.888 (□), 1.33 (■), 2 (△), and 3 mM (▲)]. (B) Double-reciprocal plot of reaction velocity versus concentration of IRAK-1 peptide. Initial rates were measured with 4 nM IRAK-4, different concentrations of the peptide, and six fixed concentrations of ATP [0.134 (○), 0.268 (●), 0.535 (□), 1.07 (■), 2.14 (△), and 4.28 mM (▲)]. The solid lines were generated by global fitting of the data to eq 2.

data, individual plots of initial rates versus concentration of the varied substrate were generated and fit to the Michaelis−Menten equation (eq 1). The resulting kinetic parameters, $V_{max}$ and $K_m$, were then used to draw lines through the data plotted in double-reciprocal (Lineweaver−Burk) format of $1/v$ versus $1/[S]$. The double-reciprocal plots with both substrates were characterized by a family of linear, nonparallel lines that converged to the left of the $y$ axis. This intersecting line pattern indicates that the IRAK-4 reaction proceeds via a sequential mechanism where binding of both substrates to the enzyme is required before release of any products. The data do not support the ping-pong mechanism, where the enzyme acts upon one substrate forming and releasing the first product of the reaction before the second substrate can be transformed. In contrast to a sequential model, the ping-pong mechanism is characterized by a set of parallel lines in double-reciprocal plots (*23*, *29*). Further confirmation of a sequential mechanism for IRAK-4 was obtained by observing a superior fit of the initial velocity data to the kinetic equation describing a sequential mechanism (eq 2) compared to that for the ping-pong kinetic model (eq 3; data not shown). Global fitting of the bisubstrate rate data to eq 2, by the method of nonlinear least-squares, yielded the Lineweaver−Burk plots in Figure 3 that are defined by a catalytic constant ($k_{cat}$) of $30 \pm 4.1\ s^{-1}$ and ATP and peptide $K_m$ values of $668 \pm 120\ \mu M$ and $852 \pm 273\ \mu M$, respectively (Table 1). In a previous study of the functional and structural properties of recombinant human IRAK-4 kinase domain (amino acids 160−460), the enzyme was found to

Table 1: Summary of Steady-State Kinetic Parameters of IRAK-4 for Phosphorylation of IRAK-1 Peptide[a]

| parameter | value | method of determination |
|---|---|---|
| $k_{cat}$ ($s^{-1}$) | $30 \pm 2.9$ | calculated |
| $K_{m(ATP)}$ ($\mu M$) | $668 \pm 120$ | measured |
| $K_{i(ATP)}$ ($\mu M$) | $418 \pm 76$ | measured |
| $k_{cat}/K_{m(ATP)}$ ($M^{-1}\ s^{-1}$) | $(4.5 \pm 0.92) \times 10^4$ | calculated |
| $K_{m(pep)}$ | $852 \pm 273$ | measured |
| $K_{i(pep)}$ | $734 \pm 444$ | measured |
| $k_{cat}/K_{m(pep)}$ ($M^{-1}\ s^{-1}$) | $(3.5 \pm 1.20) \times 10^4$ | calculated |

[a]The kinetic parameters were generated by fitting initial velocity data to the equation for a sequential kinetic mechanism (eq 2). Average values from three independent experiments with standard error for each parameter are shown. The catalytic constant, $k_{cat}$, was calculated from measured $V_{max}$ and total concentration of IRAK-4 ($k_{cat} = V_{max}/[E]$).

phosphorylate the same peptide substrate utilized in the present study with similar $K_m$ values of 650 $\mu M$ for ATP and 1100 $\mu M$ for the peptide (*14*). In contrast to the full-length enzyme, the kinase domain construct displayed a 4-fold slower turnover number ($7\ s^{-1}$).

In a bisubstrate reaction, the binding pockets for the substrates may function independently of one another or interact in a synergistic or antagonistic fashion (*23*). An examination of the Michaelis and the dissociation constants (in eq 2 $K_a$ and $K_{ia}$, respectively) revealed the α factor to be close to unity for both substrates, a finding that was interpreted as evidence for little or no interaction taking place between the substrate sites.

*ATPase Activity of IRAK-4*. In order to determine whether IRAK-4 can form a catalytically competent binary complex with ATP, we measured the ATP hydrolytic activity of the enzyme in the absence of the peptide substrate. These studies revealed that full-length IRAK-4 does possess a basal ATPase activity that is characterized by a $k_{cat}$ of $0.47 \pm 0.03\ s^{-1}$ and an ATP $K_m$ of $577 \pm 171\ \mu M$. Relative to the phosphate transfer reaction to the peptide under saturating substrate concentrations, the basal ATPase reaction is ~60-fold slower. The similarity in the ATP $K_m$ for the phosphoryl transfer reaction in the presence and absence of the peptide substrate is consistent with the finding from bisubstrate kinetic experiments that the peptide does not influence the affinity of the enzyme for ATP. The slow ATPase $k_{cat}$ together with the relatively poor affinity of the enzyme for ATP suggests that the basal ATPase reaction transpires via a rapid equilibrium mechanism where ATP is more likely to come off the enzyme than proceed forward to hydrolysis.

*Effect of Salt on Kinetic Properties of IRAK-4*. The bisubstrate kinetic experiments as well as the subsequent inhibition studies were carried out in the presence of a near physiological salt (NaCl) concentration of 170 mM. In view of the relatively high ATP and peptide $K_m$ values, as well as the charged nature of both substrates, we sought to determine if the presence of salt impacted the kinetic properties of the enzyme. To that end, apparent kinetic parameters were measured in a series of titration experiments using varying concentrations of NaCl ranging from 20 to 170 mM. The measured kinetic constants at 20 and 170 mM NaCl are summarized in Table 2. Interaction with ATP appeared to be minimally affected, as little change in its $K_m$ was noted. In contrast, a 34% reduction in $k_{cat}$ was observed in response to the increase in the concentration of NaCl from 20 to 170 mM. The biggest effect was observed on the $K_m$ for the peptide, exhibiting a 2.3-fold upward shift as the concentration of salt was raised to 170 mM.

Table 2: Effect of Salt on Kinetic Parameters of IRAK-4[a]

| kinetic parameter | 20 mM NaCl | 170 mM NaCl |
|---|---|---|
| $K_{m(ATP)}$ (mM) | 1.4 ± 0.3 | 1.2 ± 0.6 |
| $K_{m(pep)}$ (mM) | 0.7 ± 0.2 | 1.6 ± 0.4 |
| $k_{cat}$ ($s^{-1}$) | 18.1 ± 3.7 | 12.0 ± 2.1 |

[a]Initial rates were measured as a function of varying concentrations of one substrate while the second substrate was maintained at a constant, nearly saturating concentration and in the presence of different concentrations of NaCl (20, 45, 70, 120, and 170 mM). Apparent kinetic parameters were obtained by fitting the initial velocities, from at least two independent experiments, to eq 1. Results with standard deviations for the lowest and highest concentrations of NaCl are shown.

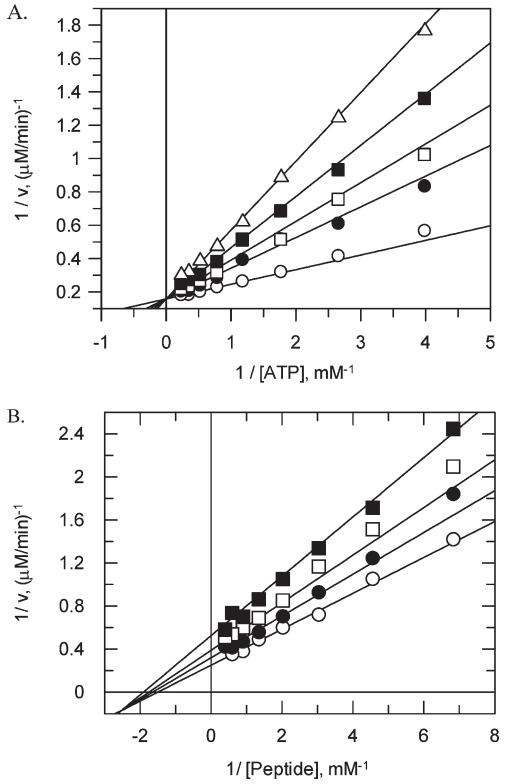


FIGURE 4: Kinetics of inhibition by AMPPNP. (A) Double-reciprocal plot of initial velocity versus concentration of ATP generated utilizing 4 nM IRAK-4, varying concentrations of ATP (0.25−4 mM), one fixed concentration of IRAK-1 peptide (1.3 mM), and different concentrations of AMPPNP [0 (○), 1.2 (●), 1.8 (□), 2.7 (■), and 4 mM (△)]. (B) Double-reciprocal plot of initial velocity versus concentration of IRAK-1 peptide generated with 4 nM IRAK-4, varying concentrations of the peptide (0.15−2.5 mM), one fixed concentration of ATP (0.8 mM), and different concentrations of AMPPNP [0 (○), 0.5 (●), 1 (□), and 2 mM (■)].

*Substrate Analogue and Product Inhibition Studies*. In a sequential kinetic mechanism the binding of substrates and release of products can occur in a specific order or in a random fashion. Inhibition studies involving dead-end substrate analogues and products of the reaction can provide clues for differentiating the possible kinetic pathways (*23*, *30*, *31*). The dead-end inhibitor, AMPPNP, behaved as a competitive inhibitor of IRAK-4 with ATP as the varied substrate (Figure 4A). Global fitting of the rate data to the equation describing competitive enzyme inhibition (eq 4) yielded an inhibition constant of 0.97 ± 0.09 mM (Table 3). Against the peptide substrate, AMPPNP acted as a noncompetitive inhibitor (Figure 4B). Fitting the rate data to the equation for noncompetitive inhibition (eq 5) yielded

Table 3: Inhibition Constant and Mechanism of Inhibition of IRAK-4 by AMPPNP and ADP[a]

| inhibitor | variable substrate | mechanism of inhibition | $K_{is}$ (mM) | $K_{ii}$ (mM) |
|---|---|---|---|---|
| AMPPNP | ATP | competitive | 0.97 ± 0.09 | |
| AMPPNP | peptide | noncompetitive | 3.62 ± 0.52 | 2.0 ± 0.4 |
| ADP | ATP | competitive | 1.63 ± 0.37 | |
| ADP | peptide | noncompetitive | 4.05 ± 0.05 | 4.8 ± 1.8 |

[a]Inhibition constants were derived by fitting initial rate data, from three independent experiments, to the equation for either competitive (eq 4) or noncompetitive inhibition (eq 5). Results with standard error of the mean are indicated.

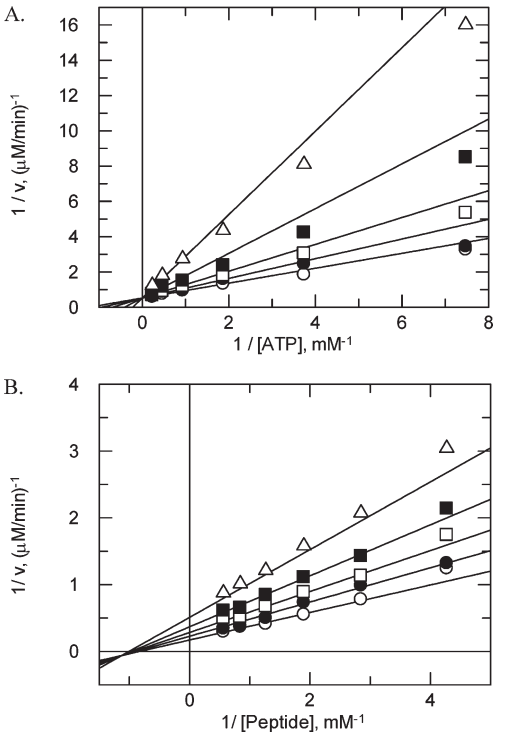


FIGURE 5: Kinetics of inhibition by ADP. (A) Double-reciprocal plot of initial velocity versus concentration of ATP. The reaction consisted of 4 nM IRAK-4, 1.3 mM peptide, varying concentrations of ATP (0.13−4.3 mM), and varying concentrations of ADP [0 (○), 0.5 (●), 1.25 (□), 3.13 (■), and 7.18 mM (△)]. (B) Double-reciprocal plot of initial velocity versus concentration of IRAK-1 peptide. The reaction included 4 nM IRAK-4, 0.8 mM ATP, varying concentrations of the peptide (0.23−1.78 mM), and varying concentrations of ADP [0 (○), 1 (●), 2 (□), 3.5 (■), and 6 mM (△)].

a $K_{is}$ (reflecting affinity of the inhibitor for free enzyme) of 3.62 ± 0.52 mM and a $K_{ii}$ (reflecting affinity of the inhibitor for enzyme−peptide complex) of 2.0 ± 0.4 mM (Table 3). The close values of $K_{is}$ and $K_{ii}$ indicated that AMPPNP does not have a preference for free enzyme versus enzyme−peptide complex or vice versa. The AMPPNP results ruled out a sequential ordered mechanism with the peptide substrate binding to the enzyme first. In this mechanism, an inhibitor analogue of ATP is predicted to show an uncompetitive mode of inhibition against the peptide.

One of the products of the reaction resulting from phosphoryl transfer activity of kinases is ADP. As shown in Figure 5, ADP was a competitive inhibitor versus ATP and a noncompetitive inhibitor against the peptide substrate. Similarly to AMPPNP, ADP interacted with IRAK-4 with poor affinity (inhibition constants in the 1.6−4.8 mM range) and exhibited similar affinity for free enzyme and the enzyme−peptide binary complex

Scheme 1


Scheme 2

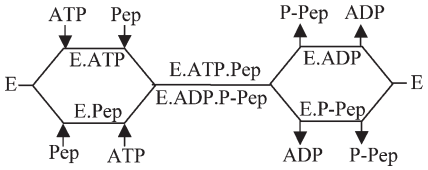


(Table 3). Overall, the inhibition pattern of IRAK-4 with the nucleotide inhibitors is consistent with both a sequential ordered mechanism (Scheme 1), with ATP binding to the enzyme prior to the peptide substrate, and a random mechanism (Scheme 2).

Previous work on phosphorylation of IRAK-1 activation loop peptides by IRAK-4 had identified Ser 376 as one of the primary phospho-acceptor residues (*2*). To further clarify the kinetic mechanism of IRAK-4, we attempted to utilize a phosphorylated peptide that carries a phosphate on an equivalent residue (Ser 17) on our substrate, as the other product of the reaction. However, several problems were encountered in using the phosphopeptide as a product inhibitor. First, when tested alone in our IRAK-4 kinase assay, we detected phosphorylation of the phosphopeptide, albeit at a lower rate (~7−12% of that observed with the unphosphorylated peptide; data not shown). The low background activity most likely arises from phosphorylation of the unmodified serine residues. These results indicated that the phosphopeptide acts as an alternative substrate and implied that, in the presence of the unmodified peptide, contribution of the phosphopeptide to the overall velocity can be significant. On the basis of these results, we deem treating the phosphopeptide as a pure product inhibitor unjustified. Even if the contribution of the phosphopeptide to the reaction velocity were to be ignored, when tested over a phosphopeptide concentration range up to 2 mM, weak inhibition of IRAK-4 at concentrations $<1$ mM and an unproportionally high degree of inhibition at 2 mM were observed (data not shown). Moreover, overall there was significant variation in the extent of inhibition from experiment to experiment (data not shown). Together, these findings precluded the use of the phosphopeptide as a product inhibitor to reach a definitive conclusion about the kinetic mechanism of IRAK-4.

*Effect of $Mg^{2+}$ on Kinase Activity of IRAK-4*. For our kinetic studies of IRAK-4, we chose $Mg^{2+}$ as it is believed, due to its high *in vivo* concentration relative to other divalent metal ions, to be the physiologically relevant metal activator of protein kinases (*32*). Steady-state kinetic properties of IRAK-4 were initially determined utilizing an arbitrary concentration of 20 mM $Mg^{2+}$. Kinetic properties of several protein kinases have been shown to change depending on the identity and concentration of the metal activator. We were interested in determining the optimum concentration of $Mg^{2+}$ for supporting IRAK-4's kinase activity and elucidating the role that the metal plays in the catalytic function of IRAK-4. Depending on the pH of the medium, ATP can exist in several ionization states that bind divalent metals with different affinities (*33*). At pH 8.0 ATP will be predominantly present in the $ATP^{4-}$ species. In order to minimize the occurrence of ionized forms of ATP other than $ATP^{4-}$ and ensure that $Mg^{2+}$ is the only ATP-binding ligand in the reaction mixture, the assay buffer was modified to 75 mM

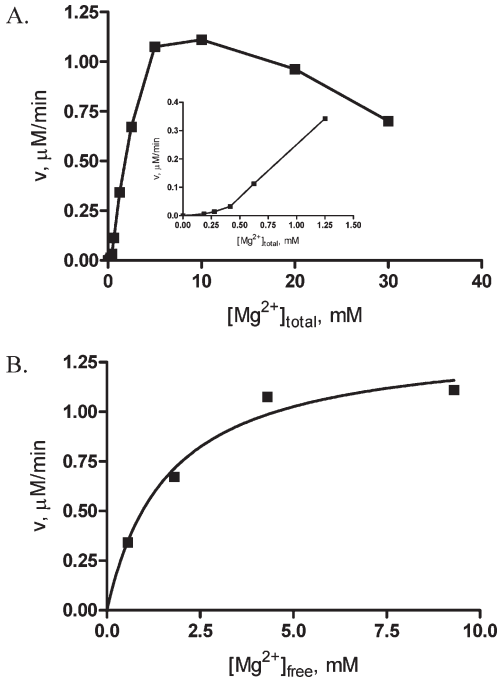


FIGURE 6: Dependence of initial velocity on the concentration of total and free $Mg^{2+}$. (A) Kinase activity of IRAK-4 (4 nM) was measured with a fixed concentration of ATP (0.7 mM) and peptide (0.5 mM), while varying the concentration of total $Mg^{2+}$ from 0.19 to 30 mM. The inset shows change in initial rates at concentrations of $Mg^{2+}$ below and slightly above the concentration of ATP. (B) Same rate data as in (A) plotted against the concentration of free $Mg^{2+}$ and fit to the equation for a rectangular hyperbola. The concentration of free $Mg^{2+}$ was calculated using the total concentrations of ATP and $Mg^{2+}$ and the quadratic form of the equation for association equilibrium between ATP and $Mg^{2+}$.

EPPS (pH 8.0), 0.01% Tween 20, and 20 mM NaCl. In a study of metal cation dependence of several Tyr-specific kinases, it had previously been shown that an EPPS-based buffer system has no Mg-binding activity (*18*). Linearity with time and concentration of IRAK-4 was shown to be maintained in the EPPS-based assay buffer (data not shown). The enzyme exhibited an almost 2-fold increase in activity relative to the standard assay buffer (data not shown). Based on our findings on the effects of salt on kinetic parameters of IRAK-4 (Table 2), at least some of the enhancement in the activity of the enzyme in the EPPS buffer can be attributed to the reduced salt concentration in the assay buffer.

Consistent with the notion that the metal complex of ATP is the true substrate in most kinase reactions, in the absence of $Mg^{2+}$, IRAK-4 failed to phosphorylate the peptide substrate (data not shown). To probe the response of reaction velocity to $Mg^{2+}$ and to shed light on the binding stoichiometry with IRAK-4, a titration experiment in which initial rates of the reaction were measured under a fixed, subsaturating concentration of each substrate (0.7 mM ATP and 0.5 mM peptide) and varying concentrations of $Mg^{2+}$ was carried out. As shown in Figure 6A, the rate of the reaction increased with concentration of total $Mg^{2+}$ reaching a maximum at a concentration range of 5−10 mM. At levels above 10 mM, the activity of the enzyme was inhibited. The association constant of the MgATP complex under conditions similar to those employed in this study has been reported to be 73 $mM^{-1}$ (*33*). Based on this value, in the titration experiment depicted in Figure 6A, ATP will titrate the $Mg^{2+}$ ions until its concentration is exceeded by that of the metal ion. After saturation of ATP, further addition of $Mg^{2+}$ will result

in an increase in the levels of free metal. At 1.25 mM total $Mg^{2+}$, approximately 98% of ATP (0.68 mM) was calculated to be in complex with the metal, and the reaction proceeded at a rate of 0.11 $\mu$M/min. An examination of Figure 6A shows that the rate of the reaction continues to increase in a $Mg^{2+}$-dependent manner even after ligation of most of ATP. At a concentration of 10 mM $Mg^{2+}$, ~93% of $Mg^{2+}$ was estimated to be in the free form, and the reaction proceeded at a maximum rate of 1.1 $\mu$M/min, which is 10 times faster than the rate at 1.25 mM metal. The increase in the activity of IRAK-4 at concentrations of $Mg^{2+}$ above that of ATP cannot be attributed to increased levels of the MgATP complex because most of the nucleotide is $Mg^{2+}$ bound at stoichiometric concentrations of the metal. This behavior suggests the presence of one or more binding site(s) for free $Mg^{2+}$ which when occupied stimulates the catalytic activity of IRAK-4. Figure 6B, generated by plotting the same rate data but as a function of concentration of free $Mg^{2+}$, as opposed to total concentration of $Mg^{2+}$, yielded a hyperbolic curve, from which an apparent $k_{cat}$ of 1.4 $s^{-1}$ and a $K_{0.5}$ of 1.6 mM for free $Mg^{2+}$ were obtained. The loss in enzyme activity at concentrations of $Mg^{2+}$ above 10 mM does not appear to be related to changes in ionic strength, because no inhibition of enzyme activity of IRAK-4 was observed with NaCl up to a concentration of 50 mM (data not shown). The inhibition may arise from free $Mg^{2+}$ forming an abortive complex with the enzyme at high concentrations, or it could be due to the presence of additional $Mg^{2+}$ binding sites with inhibitory activity. Thus, IRAK-4 appears to have at least two metal-binding sites: one for interaction with an essential $Mg^{2+}$ as part of a metal−ATP complex and a second, lower affinity regulatory site for free $Mg^{2+}$.

*Effect of Free Magnesium on the Steady-State Kinetic Parameters of IRAK-4*. The activating effect of free $Mg^{2+}$ could arise from alterations of one or more of the steady-state kinetic parameters of IRAK-4. In order to tease out the mechanism by which free $Mg^{2+}$ exerts its effect, initial rates were measured under varying concentrations of peptide and several fixed concentrations of ATP and free $Mg^{2+}$. The rate data were fit to eq 2 for a sequential kinetic mechanism. Representative double-reciprocal plots for two concentrations of free $Mg^{2+}$ (0.5 and 9 mM) are shown in Figure 7. The corresponding kinetic constants are listed in Table 4. A shift in all of the kinetic constants was observed as the concentration of free $Mg^{2+}$ was raised from 0.5 to 9 mM. The changes included an ~3-fold improvement in $k_{cat}$ and $K_m$ for MgATP and a 2- and 10-fold increase in peptide $K_m$ and $K_d$, respectively. At 0.5 mM, the calculated α factor for interaction of the peptide with the enzyme was 10, and the Lineweaver−Burk pattern was intersecting in the third quadrant. These observations suggest that when the enzyme is not saturated with free $Mg^{2+}$, MgATP and peptide binding sites interact with significant negative cooperativity. In contrast, at 9 mM $Mg^{2+}$, the two substrate sites are noninteracting as indicated by an α factor of 1 and a line pattern in the double-reciprocal plot that converges on the *x* axis (Figure 7B and Table 4). Figure 8 shows how the various kinetic parameters change over the range of free $Mg^{2+}$ concentrations used in these experiments. The apparent affinity for the peptide decreased slightly as the concentration of $Mg^{2+}$ was raised, although due to the scatter of the data the trend was not obvious. In contrast, a clear decreasing trend for ATP $K_m$ versus concentration of free $Mg^{2+}$ was observed. A fit of the apparent ATP $K_m$ values to eq 7 yielded a $K_{MgATP}$ ($K_m$ for MgATP in the absence of free $Mg^{2+}$) of 2.5 ± 0.2 mM, a $K_{MgATP''}$ ($K_m$ for MgATP with saturating free $Mg^{2+}$) of 0.25 ± 0.15 mM and a dissociation constant for $Mg^{2+}$ of 1.8 ± 0.6 mM. As determined from a fit to a hyperbolic function in Figure 8C, free $Mg^{2+}$ activates $k_{cat}$ to a maximum value of 32.5 $s^{-1}$ with half-maximal activation occurring at a metal concentration of 1.1 ± 0.3 mM. The $Mg^{2+}$ $K_{0.5}$ obtained from the $k_{cat}$ response curve is close to the dissociation constant obtained from the analysis of the effects of free $Mg^{2+}$ on ATP $K_m$. Overall, it appears that free $Mg^{2+}$, within a narrow concentration range, stimulates the catalytic activity of IRAK-4 by lowering the $K_m$ for ATP and enhancing the rate of turnover.

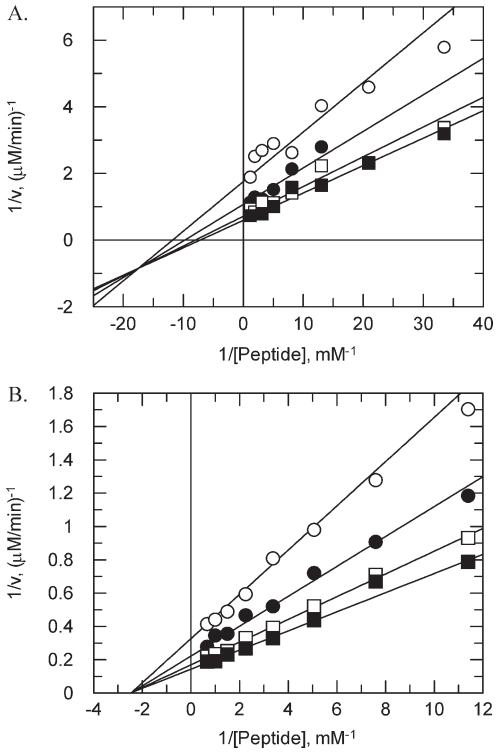


FIGURE 7: Two-substrate kinetic results with varying concentrations of free $Mg^{2+}$. In (A) four fixed concentrations of ATP [0.6 (○), 1.2 (●), 2.5 (□), and 4 mM (■)], varying concentrations of the peptide (0.03−0.8 mM), and a constant concentration of free $Mg^{2+}$ (0.5 mM) were used. In (B) four fixed concentrations of ATP [0.37 (○), 0.75 (●), 1.5 (□), and 3 mM (■)], varying concentrations of the peptide (0.09−1.5 mM), and a constant concentration of free $Mg^{2+}$ (9 mM) were used. The lines were generated by nonlinear least-squares fitting of initial velocities to eq 2 with peptide as the varied substrate.

Table 4: Steady-State Kinetic Constants of IRAK-4 at Two Different Concentrations of Free $Mg^{2+}$[a]

| kinetic parameter | 0.5 mM $Mg^{2+}$ | 9 mM $Mg^{2+}$ |
|---|---|---|
| $k_{cat}$ ($s^{-1}$) | 10.5 ± 0.7 | 31.2 ± 3 |
| $K_{m(ATP)}$ (mM) | 2.0 ± 0.1 | 0.7 ± 0.06 |
| $K_{m(pep)}$ (mM) | 0.15 ± 0.03 | 0.35 ± 0.03 |
| $K_{i(pep)}$ (mM) | 0.03 ± 0.008 | 0.35 ± 0.05 |

[a]Initial velocities were measured at varying concentrations of peptide and different, fixed concentrations of ATP. With 0.5 mM $Mg^{2+}$, peptide concentration was varied in the range of 0.03−1.5 mM. With 9 mM $Mg^{2+}$, slightly higher concentrations of the peptide (0.09−2 mM) were used. ATP concentration ranged from 0.38 to 6 mM. Kinetic constants resulting from fitting the rate data to the equation for a ternary kinetic mechanism (eq 2), along with standard error of the mean for at least three independent measurements, are shown.

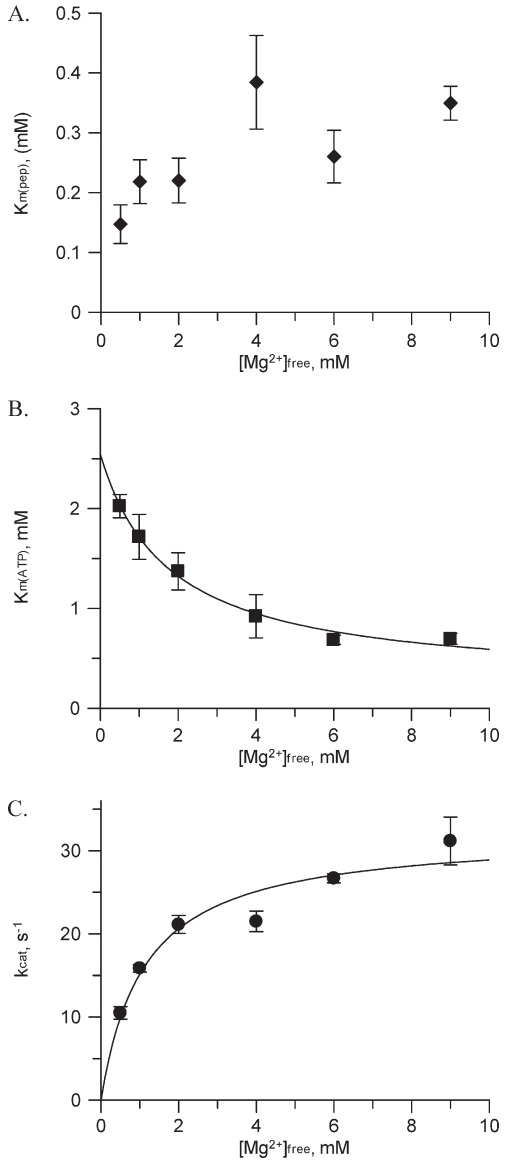


FIGURE 8: Variation in steady-state kinetic parameters of IRKA-4 as a function of the concentration of free $Mg^{2+}$. As presented in Figure 7, initial rates were measured utilizing varying concentrations of the peptide, several fixed concentrations of ATP, and several different concentrations of free $Mg^{2+}$. Kinetic constants were generated by fitting initial velocities to eq 2. (A, B) Dependence of peptide and ATP $K_m$ on the concentration of free $Mg^{2+}$, respectively. Equation 7 was used to draw the line in (B). (C) Variation in $k_{cat}$ in response to changing concentrations of free metal. The line is from a fit of $k_{cat}$ constants at each concentration of free $Mg^{2+}$ to the equation for a rectangular hyperbola.

## DISCUSSION

IRAK-4 is a Ser/Thr protein kinase that plays an indispensable role in signal transmission from the membrane to intracellular targets in the TLR/IL-1R signaling cascades. Following activation of its cognate receptors *in vivo*, IRAK-4 acts upon IRAK-1, phosphorylating it on residues in the activation loop (*10*). The studies presented here entailed a detailed kinetic characterization of the phosphoryl transfer activity of IRAK-4 toward a peptide substrate derived from the activation loop of IRAK-1. In addition to determining the kinetic constants for this reaction, we demonstrated that IRAK-4 obeys a sequential kinetic pathway. Our kinetic data are consistent with both a strictly ordered mechanism, in which ATP binds to IRAK-4 before the peptide, and a random mechanism. Divalent metals are required for the phosphoryl transfer activity of most kinases. We sought to define the role that $Mg^{2+}$ plays in the catalytic function of IRAK-4 and elucidate the mechanism by which catalysis is modulated by this metal cation. These studies revealed that IRAK-4 requires more than one $Mg^{2+}$ for optimum activity and that free $Mg^{2+}$ enhances catalytic activity of IRAK-4 by increasing the rate of substrate turnover and by reducing the $K_m$ for ATP.

IRAK-4 is the most receptor-proximal kinase yet identified in the TLR/IL-1R signaling pathways. Association with ligated receptors results in activation of IRAK-4 by a mechanism that is thought to involve autocatalyzed phosphorylation of the activation loop. Confirming earlier findings by Cheng et al. (*16*), we show here that purified, full-length recombinant IRAK-4 undergoes activation in the presence of MgATP and that the kinase activity of the enzyme is maximally realized when the enzyme is preexposed to ATP and $Mg^{2+}$ (Figure 1). When the enzyme is not pretreated with MgATP, a lag in progress curves was evident (Figure 1A). Peptide phosphorylation during the lag phase was estimated to proceed at a rate 10−20-fold slower than the rate of the reaction posttreatment with ATP and $Mg^{2+}$. This 10−20-fold difference in rate, however, is likely a lower estimate of the degree of activation of IRAK-4, because the enzyme has probably undergone partial activation during the lag phase. In their investigation of the mechanism of activation of *in vitro* activated IRAK-4 and IRAK-4 transiently expressed in HEK293 cells, Cheng and co-workers identified three sites in the activation loop (Thr 342, Thr 345, and Ser 346) that are autophosphorylated via an intramolecular mechanism. If activation of native IRAK-4 *in vivo* occurs intramolecularly, it is not clear how its recruitment to the induced receptor complex would enhance that process. As speculated by Cheng et al., one possibility is that localization to the activated receptor exposes IRAK-4 to a factor(s) that promotes the autoactivation reaction by, for instance, inducing a conformational change in IRAK-4 that allows the autophosphorylation to proceed with greater efficiency. In resting cells, IRAK-1 is bound up in a complex with a protein called Tollip that presumably blocks activation and autophosphorylation of IRAK-1 (*34*) Localization of IRAK-1 to the induced-receptor complex has the dual effect of mitigating this inhibition and bringing IRAK-1 and its activating kinase, IRAK-4, into close proximity. A similar mechanism involving association with an inhibitory factor may keep cytoplasmic IRAK-4 in uninduced cells in a functionally repressed state. Further functional and structural studies utilizing mutant forms of IRAK-4 that lack autophosphorylation activity are needed for deciphering the mechanism of activation of IRAK-4 in cells.

Aside from the limited kinetic data provided in the report by Cheng et al., the kinetic mechanism of IRAK-4 had remained poorly characterized prior to the studies presented herein. As a first step toward a better understanding of IRAK-4's enzyme mechanism, we measured its steady-state kinetic parameters (Table 1). A cursory survey of the published kinetic parameters for several protein kinases showed that, in comparison to other kinases, while IRAK-4 has a robust catalytic constant, its substrate $K_m$ values are among the highest. Furthermore, the calculated second-order rate constants ($k_{cat}/K_m$) are far from the upper limits of diffusion-controlled rates of enzyme and substrate combination (*35*). Similar to full-length IRAK-4, a truncated kinase domain construct (amino acids 160−460) of IRAK-4 was found to phosphorylate the IRAK-1 peptide substrate with low efficiency as evident by apparent $K_m$ values of 650 and 1100 $\mu$M

and apparent $k_{cat}/K_m$ constants of $1.1 \times 10^4$ and $0.6 \times 10^4$ $M^{-1}$ $s^{-1}$ for ATP and the peptide, respectively (*14*). In contrast to full-length IRAK-4, however, the kinase domain displayed an ~4-fold slower turnover number of 7 $s^{-1}$.

The kinetic parameters determined for full-length IRAK-4 in this study (Table 1) were found to be significantly different from those reported by Cheng and co-workers (apparent ATP $K_m$ of 24.4 $\mu$M and $k_{cat}$ of 2.24 $s^{-1}$ (*16*)). At this point, it is not clear why such significant discrepancies exist between the two studies. In both studies, the enzyme was purified to greater than 90% homogeneity and activated by treatment with ATP and $Mg^{2+}$. The phosphorylation pattern of activated IRAK-4 generated in the present study was not profiled, raising the possibility that even though similar experimental conditions were used to activate the enzyme in the two studies, the enzyme was differentially phosphorylated and as a result exhibits different kinetic properties. Another important difference between the two studies has to do with the components of the kinase assays. The most potentially consequential differences include the sequence and size of the peptide substrate, the ionic strength of the reaction medium (presence of 170 mM NaCl in our assay buffer versus a salt-free buffer used by Cheng et al.), and the choice and concentration of the divalent cation (20 mM $Mg^{2+}$ used in this study as opposed to 2 mM $Mn^{2+}$ utilized by Cheng et al.). In studies probing polypeptide substrate specificity of several protein kinases, the identity of the phospho-acceptor substrate has been documented to make a difference in the steady-state kinetic properties of the enzyme (*36*−*38*). It may be that the kinetics of IRAK-4 is also prone to change depending on the nature of the phospho-acceptor substrate. It would be interesting to examine the kinetic properties of IRAK-4 with one of its whole protein, *in vivo* substrates such as IRAK-1. In our investigation of the basal rate of hydrolysis of ATP by IRAK-4, we discovered an ATP $K_m$ of 577 $\mu$M, which is similar to the corresponding value for the phosphoryl transfer activity with the peptide substrate (Table 1). This suggests that the IRAK-1 peptide, as also evidenced by the bisubstrate kinetic results, does not adversely affect the interaction of IRAK-4 with ATP. The question of cooperativity between substrate sites was not probed in the study by Cheng and co-workers. As shown in Table 2, NaCl, at the highest concentration (170 mM) used in our standard assay, has little impact on the kinetic constants and thus did not seem to be a factor contributing to the differences observed in the two studies. Several studies have demonstrated alteration of steady-state kinetic parameters of protein kinases in a manner dependent on the type and concentration of the metal cation. A discussion of the effects of concentration of $Mg^{2+}$ on the kinetic properties of IRAK-4 will be presented in the following sections.

In addition to determining the kinetic constants defining the IRAK-4 reaction, we were interested in establishing the kinetic pathway by which the reaction proceeds. On the basis of the results from the bisubstrate kinetic studies and the inhibition profile observed with AMPPNP, we were able to infer a sequential pathway for IRAK-4 and rule out two mechanisms, the strictly ordered mechanism with the peptide binding to the enzyme before ATP and the rapid-equilibrium ordered with ATP binding first to the enzyme (Figure 3 and Table 3). The rationale for ruling out the strictly ordered mechanism with the peptide binding first to the enzyme was presented in the Results section. If the IRAK-4 reaction obeyed a rapid-equilibrium ordered mechanism with ATP binding prior to the peptide, then $V_{max}$ should exhibit no dependence on the concentration of ATP when the peptide is the varied substrate. The reason for this is that, at very high peptide substrate concentrations, the equilibrium between ATP and free enzyme will be shifted to the bound complex, and because the concentration of the nucleotide is in vast excess of that of the enzyme, no change in the concentration of the enzyme−ATP complex would be expected as the concentration of ATP is changed. As a result, the lines in the plot of $1/v$ versus 1/[peptide] should intersect on the $y$ axis. Moreover, a secondary plot of slope versus concentration of ATP should go through the origin (*23*). Neither one of these predictions is fulfilled by the results of our kinetic studies. The double-reciprocal lines clearly intersect behind the $y$ axis (Figure 3), and the secondary plots of slope versus concentrations of the fixed substrate yielded linear lines that cross the $y$ axis above the origin (data not shown). Together, the AMPPNP and ADP inhibition results are most consistent with either a steady-state ordered mechanism in which ATP is the first substrate to add or a random mechanism that includes an abortive complex consisting of enzyme, peptide, and ADP (Schemes 1 and 2, respectively).

ADP inhibited IRAK-4 weakly with an inhibition constant in the low millimolar range (Table 3). This high inhibition constant is indicative of a low affinity interaction between IRAK-4 and ADP that we speculate is due to a rapid rate of dissociation. The affinity of the phosphopeptide (the other product of the reaction) is unknown. But, considering the relatively high dissociation constant of the peptide substrate, it seems reasonable to also assume a poor affinity interaction between IRAK-4 and the phosphopeptide and a fast off rate for its release from the enzyme. On the basis of the above considerations, we propose that in the IRAK-4-catalyzed phosphorylation reaction of IRAK-1 peptide, the phosphoryl transfer step is at least partially rate limiting.

With the exception of CASK ($Ca^{2+}$/calmodulin activated Ser/Thr kinase), free ATP does not serve as a substrate in protein kinase-catalyzed phosphoryl transfer reactions (*39*). The results of the studies presented here and those of Cheng et al. (*15*) show that catalytic activity of IRAK-4 requires divalent metal cations. The most abundant divalent cation in the cell is $Mg^{2+}$. This predominance of $Mg^{2+}$ over other divalent cations led us to choose it as the activator of IRAK-4 in our kinase assays. To shed light on the role(s) that $Mg^{2+}$ plays in the catalytic function of IRAK-4, we examined its effect on the kinetics of the reaction. In a titration experiment examining the sensitivity of initial velocities to concentration of $Mg^{2+}$, the activity of the enzyme was observed to increase with levels of total $Mg^{2+}$ above what is needed to drive most of ATP into the metal chelate complex (Figure 6A). At higher metal concentrations a drop in the activity of the enzyme was noted. As indicated in the inset in Figure 6A, in the noninhibitory concentration range of total $Mg^{2+}$, reaction velocity exhibited a slow rise over substoichiometric concentrations of $Mg^{2+}$, relative to the concentration of ATP, followed by a more steep increase as levels of $Mg^{2+}$ exceeded the concentration of ATP. Thus, at least qualitatively, initial velocities appeared to change in a sigmoidal fashion with the concentration of $Mg^{2+}$. Moving up the titration curve, as the concentration of $Mg^{2+}$ approaches that of ATP, the levels of both MgATP and free $Mg^{2+}$ rise, resulting in an increase in the rate of turnover. The additional increase in reaction velocity with concentration of $Mg^{2+}$ after saturation of ATP implies the presence of at least a second metal-binding site on the enzyme. The mechanism of activation by free $Mg^{2+}$ does not appear to be due to changes in the ionic strength because reaction rate remains stable under

increasing concentrations of NaCl up to 50 mM and shows a decrease at higher levels (Table 2). Also, the increase in the activity of the enzyme in the presence of free $Mg^{2+}$ does not seem to arise from increased stability of the enzyme because the enzyme, as evidenced by linear progress curves, tends to be fairly stable under a variety of experimental conditions (data not shown). On the basis of the data presented here, we propose the presence of at least one activating regulatory site for free $Mg^{2+}$ in IRAK-4 and possibly one or more additional weaker affinity binding sites that suppress the activity of the enzyme.

The mechanism by which divalent metals modulate kinetics of kinases has been probed by a variety of approaches. Among Ser/Thr kinases, one of the best characterized cases is cAMP-activated protein kinase (PKA), where a combination of electron paramagnetic resonance, X-ray diffraction, and enzyme kinetic data has provided a detailed picture of how $Mg^{2+}$ affects the activity of this kinase (*21*, *41*). PKA has two metal binding sites. One metal ion, as part of a nucleotide chelate complex, is essential for catalysis. It interacts with high affinity with PKA (dissociation constant of ~10 $\mu$M) coordinating with $\beta$- and $\gamma$-phosphates of the nucleotide and a conserved active site Asp. The second, uncomplexed $Mg^{2+}$ binds substantially more weakly (~2 mM dissociation constant) and coordinates the α- and $\gamma$-phosphates of the nucleotide. Functionally, the second $Mg^{2+}$ was initially reported to inhibit the catalytic activity of PKA. However, subsequent and more detailed kinetic analysis showed that it has a complex kinetic effect in that it decreases both the $k_{cat}$ and $K_m$ for ATP (*21*). Thus, at saturating ATP concentrations, the second $Mg^{2+}$ has an inhibitory effect but at limiting nucleotide concentrations a stimulatory effect. CDK4, a cyclin-dependent, Ser/Thr kinase, also undergoes metal-dependent activation that entails a lowering of ATP $K_m$ without alteration of $V_{max}$ (*42*). Free $Mg^{2+}$ facilitates both ATP binding and phosphoryl transfer in ERK2 (*40*). The effect of free metal ion on several Tyr protein kinases also has been studied. With v-Fps, a nonreceptor Tyr kinase, uncomplexed $Mg^{2+}$ behaves as a nonessential activator that does not impact apparent $V_{max}$ or $K_m$ of the phospho-acceptor substrate but increases the affinity of the enzyme for MgATP by dramatically lowering its dissociation constant (*24*). In contrast to v-Fps, Csk and Src appear to require two metals for catalysis with free metal increasing both the $V_{max}$ and peptide substrate $K_m$ (*18*). In the receptor Tyr kinase family, yet another pattern of kinetic effects has been observed. In the cases of IRK and FGFR, free metal overall has an activating effect due to a heightened $V_{max}$ and lowered ATP $K_m$ offsetting an increase in the $K_m$ for the phospho-acceptor substrate (*18*). With the exception of PKA, where $k_{cat}$ is reduced, and V-Fps, where it shows no change, other protein kinases show an enhanced rate of substrate turnover in response to increasing levels of free metal. Thus, it appears that while all protein kinases, examined to date, tend to get activated by free divalent metal, they show diversity in the mechanism by which the activation occurs.

In the case of IRAK-4, $Mg^{2+}$ stimulates its kinase activity by promoting binding of ATP and increasing the catalytic constant. Moreover, free $Mg^{2+}$ was found to render the interaction between ATP and peptide binding pockets in IRAK-4 less antagonistic as evidenced by a large shift in the α factor for the peptide, from a value of 10 at 0.5 mM free $Mg^{2+}$ to 1 at 9 mM free metal. Thus, in the absence of free metal, binding of one substrate adversely affects binding of the second substrate, whereas in the presence of free $Mg^{2+}$, little interaction occurs between the two substrates. Within the available data set, IRAK-4 resembles more closely receptor Tyr kinases with respect to the kinetic effects of free metal activation. Interestingly, in phylogenetic analysis, IRAK-4 groups with Tyr kinases, and as pointed out by Wang et al., IRAK-4 resembles more closely Tyr kinases in its pattern of interactions involving phosphorylated residues in its activation loop (*15*, *43*). The steady-state kinetic constants of a multisubstrate reaction are complex parameters and are often comprised of several microscopic rate constants. Other approaches such as transient kinetic methodologies are needed to identify the step(s) in the catalytic pathway of IRAK-4 that is affected by free $Mg^{2+}$ and determine the magnitude of the change in the corresponding rate constants. Also, X-ray resolved structures of nucleotide-ligated IRAK-4 at higher resolution around the active pocket than the currently available structures are needed to reveal if IRAK-4 diverges from other kinases in its pattern of metal coordination.

## ACKNOWLEDGMENT

We express our gratitude to Stan Tsing and Kyung Song for providing us with purified, activated IRAK-4 protein and to Holly Fleshman for reading the manuscript.

## REFERENCES

1. Janssens, S., and Beyaert, R. (2003) Functional diversity and regulation of different interleukin-1 receptor-associated kinase (IRAK) family members. *Mol. Cell 11*, 293–302.
2. Li, S., Strelow, A., Fontana, E. J., and Wesche, H. (2002) IRAK-4: a novel member of the IRAK family with the properties of an IRAK-kinase. *Proc. Natl. Acad. Sci. U.S.A. 99*, 5567–5572.
3. Picard, C., Puel, A., Bonnet, M., Ku, C. L., Bustamante, J., Yang, K., Soudais, C., Dupuis, S., Feinberg, J., Fieschi, C., Elbim, C., Hitchcock, R., Lammas, D., Davies, G., Al-Ghonaium, A., Al-Rayes, H., Al-Jumaah, S., Al-Hajjar, S., Al-Mohsen, I. Z., Frayha, H. H., Rucker, R., Hawn, T. R., Aderem, A., Tufenkeji, H., Haraguchi, S., Day, N. K., Good, R. A., Gougerot-Pocidalo, M. A., Ozinsky, A., and Casanova, J. L. (2003) Pyogenic bacterial infections in humans with IRAK-4 deficiency. *Science 299*, 2076–2079.
4. Suzuki, N., Suzuki, S., Duncan, G. S., Millar, D. G., Wada, T., Mirtsos, C., Takada, H., Wakeham, A., Itie, A., Li, S., Penninger, J. M., Wesche, H., Ohashi, P. S., Mak, T. W., and Yeh, W. C. (2002) Severe impairment of interleukin-1 and Toll-like receptor signaling in mice lacking IRAK-4. *Nature 416*, 750–754.
5. Lye, E., Mirtsos, C., Suzuki, N., Suzuki, S., and Yeh, W. C. (2004) The role of interleukin 1 receptor-associated kinase-4 (IRAK-4) kinase activity in IRAK-4-mediated signaling. *J. Biol. Chem. 279*, 40653–40658.
6. Medvedev, A. E., Thomas, K., Awomoyi, A., Kuhns, D. B., Gallin, J. I., Li, X., and Vogel, S. N. (2005) Cutting edge: expression of IL-1 receptor-associated kinase-4 (IRAK-4) proteins with mutations identified in a patient with recurrent bacterial infections alters normal IRAK-4 interaction with components of the IL-1 receptor complex. *J. Immunol. 174*, 6587–6591.
7. Wietek, C., and O'neill, L. A. (2002) IRAK-4: a new drug target in inflammation, sepsis, and autoimmunity. *Mol. Interv. 2*, 212–215.
8. Powers, J. P., Li, S., Jaen, J. C., Liu, J., Walker, N. P. C., Wang, Z., and Wesche, H. (2006) Discovery and initial SAR of inhibitors of interleukin-1 receptor-associated kinase-4. *Bioorg. Med. Chem. Lett. 16*, 2842–2845.
9. Burns, K., Janssens, S., Brissoni, B., Olivos, N., Beyaert, R., and Tschopp, J. (2003) Inhibition of interleukin 1 receptor/Toll-like receptor signaling through the alternatively spliced, short form of MyD88 is due to its failure to recruit IRAK-4. *J. Exp. Med. 197*, 263–268.
10. Cao, Z., Henzel, W. J., and Gao, X. (1996) IRAK: a kinase associated with the interleukin-1 receptor. *Science 271*, 1128–1131.
11. Koziczak-Holbro, M., Joyce, C., Glück, A., Kinzel, B., Müller, M., Tschopp, C., Mathison, J. C., Davis, C. N., and Gram, H. (2007) IRAK-4 kinase activity is required for interleukin-1 (IL-1) receptor- and Toll-like receptor 7-mediated signaling and gene expression. *J. Biol. Chem. 282*, 13552–13560.
12. Qin, J., Jiang, Z., Qian, Y., Casanova, J. L., and Li, X. (2004) IRAK4 kinase activity is redundant for interleukin-1 (IL-1) receptor-associated kinase phosphorylation and IL-1 responsiveness. *J. Biol. Chem. 279*, 26748–26753.

13. Song, K. W., Talamas, F. X., Suttmann, R. T., Olson, P. S., Barnett, J. W., Lee, S. W., Thompson, K. D., Jin, S., Hekmat-Nejad, M., Cai, T. Z., Manning, A. M., Hill, R. J., and Wong, B. R. (2009) The kinase activities of interleukin-1 receptor associated kinase (IRAK)-1 and 4 are redundant in the control of inflammatory cytokine expression in human cells. *Mol. Immunol. 46*, 1458–1466.
14. Kuglstatter, A., Villaseñor, A. G., Shaw, D., Lee, S. W., Tsing, S., Niu, L, Song, K. W., Barnett, J. W., and Browner, M. F. (2007) Cutting Edge: IL-1 receptor-associated kinase 4 structures reveal novel features and multiple conformations. *J. Immunol. 178*, 2641–2645.
15. Wang, Z., Liu, J., Sudom, A., Ayres, M., Li, S., Wesche, H., Powers, J. P., and Walker, N. P. (2006) Crystal structures of IRAK-4 kinase in complex with inhibitors: a serine/threonine kinase with tyrosine as a gatekeeper. *Structure 14*, 1835–1844.
16. Cheng, H., Addona, T., Keshishian, H., Dahlstrand, E., Lu, C., Dorsch, M., Li, Z., Wang, A., Ocain, T. D., Li, P., Parsons, T. F., Jaffee, B., and Xu, Y. (2007) Regulation of IRAK-4 kinase activity via autophosphorylation within its activation loop. *Biochem. Biophys. Res. Commun. 352*, 609–616.
17. Adams, J. A., and Taylor, S. S. (1993) Divalent metal ions influence catalysis and active-site accessibility in the cAMP-dependent protein kinase. *Protein Sci. 2*, 2177–2186.
18. Sun, G., and Budde, R. J. (1997) Requirement for an additional divalent metal cation to activate protein tyrosine kinases. *Biochemistry 36*, 2139–2146.
19. Sun, G., and Budde, R. J. (1999) Substitution studies of the second divalent metal cation requirement of protein tyrosine kinase CSK. *Biochemistry 38*, 5659–5665.
20. Grace, M. R., Walsh, C. T., and Cole, P. A. (1997) Divalent ion effects and insights into the catalytic mechanism of protein tyrosine kinase Csk. *Biochemistry 36*, 1874–1881.
21. Adams, J. A. (2001) Kinetic and catalytic mechanisms of protein kinases. *Chem. Rev. 101*, 2271–2290.
22. Cook, P. F., Neville, M. E., Jr., Vrana, K. E., Hartl, F. T., and Roskoski, R., Jr. (1982) Adenosine cyclic 3′,5′-monophosphate dependent protein kinase: kinetic mechanism for the bovine skeletal muscle catalytic subunit. *Biochemistry 21*, 5794–5799.
23. Segel, I. H. (1975) Enzyme Kinetics, John Wiley & Sons, Inc., New York, NY.
24. Saylor, P., Wang, C., Hirai, T. J., and Adams, J. A. (1998) A second magnesium ion is critical for ATP binding in the kinase domain of the oncoprotein v-Fps. *Biochemistry 37*, 12624–12630.
25. Wu, H., and Wang, Z. X. (2003) The mechanism of p21-activated kinase 2 autoactivation. *J. Biol. Chem. 278*, 41768–41778.
26. Parast, C. V., Mroczkowski, B., Pinko, C., Misialek, S., Khambatta, G., and Appelt, K. (1998) Characterization and kinetic mechanism of catalytic domain of human vascular endothelial growth factor receptor-2 tyrosine kinase (VEGFR2 TK), a key enzyme in angiogenesis. *Biochemistry 37*, 16788–16801.
27. Robbins, D. J., Zhen, E., Owaki, H., Vanderbilt, C. A., Ebert, D., Geppert, T. D., and Cobb, M. H. (1993) Regulation and properties of extracellular signal-regulated protein kinases 1 and 2 in vitro. *J. Biol. Chem. 268*, 5097–5106.
28. Dinh, M., Grunberger, D., Ho, H., Tsing, S. Y., Shaw, D., Lee, S., Barnett, J., Hill, R. J., Swinney, D. C., and Bradshaw, J. M. (2007) Activation mechanism and steady state kinetics of Bruton′s tyrosine kinase. *J. Biol. Chem. 282*, 8768–8776.
29. Fromm, H. J. (1979) Summary of kinetic reaction mechanisms. *Methods Enzymol. 63*, 42–53.
30. Rudolph, F. B. (1979) Product inhibition and abortive complex formation. *Methods Enzymol. 63*, 411–436.
31. Fromm, H. J. (1979) Use of competitive inhibitors to study substrate binding order. *Methods Enzymol. 63*, 467–486.
32. Romani, A., and Scarpa, A. (1992) Regulation of cell Magnesium. *Arch. Biochem. Biophy 298*, 1–12.
33. O'Sullivan, W. J., and Smithers, G. W. (1979) Stability constants for biologically important metal-ligand complexes. *Methods Enzymol. 63*, 294–336.
34. Burns, K., Clatworthy, J., Martin, L., Martinon, F., Plumpton, C., Maschera, B., Lewis, A., Ray, K., Tschopp, J., and Volpe, F. (2000) Tollip, a new component of the IL-1RI pathway, links IRAK to the IL-1 receptor. *Nat. Cell Biol. 2*, 346–351.
35. Fersht, A. (1985) Enzyme Structure and Mechanism. W. H. Freeman and Company, New York, NY.
36. Chen, G., Porter, M. D., Bristol, J. R., Fitzgibbon, M. J., and Pazhanisamy, S. (2000) Kinetic mechanism of the p38-alpha MAP kinase: phosphoryl transfer to synthetic peptides. *Biochemistry 39*, 2079–2087.
37. Czerwinski, R., Aulabaugh, A., Greco, R. M., Olland, S., Malakian, K., Wolfrom, S., Lin, L., Kriz, R., Stahl, M., Huang, Y., Liu, L., and Chaudhary, D. (2005) Characterization of protein kinase C theta activation loop autophosphorylation and the kinase domain catalytic mechanism. *Biochemistry 44*, 9563–9573.
38. Hawkins, J., Zheng, S., Frantz, B., and LoGrasso, P. (2000) p38 map kinase substrate specificity differs greatly for protein and peptide substrates. *Arch. Biochem. Biophy 382*, 310–313.
39. Mukherjee, K., Sharma, M., Urlaub, H., Bourenkov, G. P, Jahn, R., Südhof, T. C., and Wahl, M. C. (2008) CASK functions as a $Mg^{2+}$-independent neurexin kinase. *Cell 133*, 328–339.
40. Waas, W. F., and Dalby, K. N. (2003) Physiological concentrations of divalent magnesium ion activate the serine/threonine specific protein kinase ERK2. *Biochemistry 42*, 2960–2970.
41. Armstrong, R. N., Kondo, H., Granot, J., Kaiser, E. T., and Mildvan, A. S. (1979) Magnetic resonance and kinetic studies of the manganese-(II) ion and substrate complexes of the catalytic subunit of adenosine 3′,5′-monophosphate dependent protein kinase from bovine heart. *Biochemistry 18*, 1230–1238.
42. Tian, G., Kane, L. S., Holmes, W. D., and Davis, S. T. (2002) Modulation of cyclin-dependent kinase 4 by binding of magnesium (II) and manganese (II). *Biophys. Chem. 95*, 79–90.
43. Manning, G., Whyte, D. B., Martinez, R., Hunter, T., and Sudarsanam, S. (2002) The protein kinase complement of the human genome. *Science 298*, 1912–1934.